Supporting Information

Surface Band Bending Influences the Open-Circuit Voltage of Perovskite Solar Cells

Hao Hu[†]*, Susanne Birkhold*[†]*, Muhammad Sultan*[‡]*, Azhar Fakharuddin*[§]*, Susanne Koch*[†]*, and Lukas Schmidt-Mende*[†]***

[†] Department of Physics, University of Konstanz, Konstanz 78457, Germany.

[‡] Nanoscience and Technology Department, National Centre for Physics, Quaid-I-Azam University Campus, Islamabad 45320, Pakistan.

[§] IMEC, Kapeldreef 75, Heverlee 3001, Belgium.

*E-mail: Lukas.Schmidt-mende@uni-konstanz.de

Perovskite devices fabrication： ITO-coated glass substrates (15 Ω, Lumtec) were ultrasonic cleaned for 15 min by detergent, acetone and isopropanol successively. Then they were treated with oxygen plasma for 7 min. After that, around 30 nm PEDOT:PSS (Clevios™ VP AI 4083) film was spin-coated on top and then annealed at 180 ºC for 5 min. For the poly[bis(4-phenyl)(2,4,6-trimethylphenyl)amine] (PTAA, Ossila), 1.5 mg/mL solution in toluene (Sigma-Aldrich) was prepared. Around 12 nm PTAA film was deposited and annealed at 110 ºC for 10 min. Then the substrates were transferred to a glovebox where moisture and oxygen level were both lower than 5 ppm. A 40% weight ratio perovskite precursor solution was prepared by mixing

methylammonium iodide (MAI, Dyenamo), PbI_2 (Sigma-Aldrich) and $PbCl_2$ (Sigma-Aldrich) by a molar ratio of 4:1:1 in DMF:DMSO (Sigma-Aldrich) mixture (20:1) solvent. After stirring overnight, the precursor solution was spin-coated on the substrates at 3000 rpm for 20 s. Then the films were transferred immediately to a vacuum chamber with a pressure of around 1.5 mbar on a 80 ºC hotplate for 15 min. Afterwards, the films were annealed further at ambient pressure. 90-in sample was annealed under a petri dish at 90 ºC for 30 min, 90-out sample was annealed without petri dish at 90 ºC for 30 min, and 100-out sample was annealed without petri dish at 100 ºC for 30 min. Finally 20 nm C_{60} layer, 1 nm LiF layer and 60 nm Ag back contact were thermally evaporated consecutively on top of the spin-coated perovskite film to complete the device.

J-V related measurement： J−V measurements were performed using a Keithley 2400 Source Meter controlled through a self-written Matlab program in the golvebox. Cells were illuminated via a LOT 300 W Xenon solar simulator through a shadow mask with a resulting active area of 0.133 cm^2. For light-intensity dependent measurement, a series of neutral-density filters (Thorlabs) were used to adjust the illumination intensity. And light intensities were calibrated with a certified Si reference solar cell (Fraunhofer Institute) with a KG5 filter. For transient ionic current measurement, the device samples were biased at 0 V for 60 s, 0.9 V for 60 s and 0 V for 120 s in turn without illumination. The current decay in the third bias regime was integrated to calculate the corresponding ionic charge density.

Scanning electron microscopy: The morphology of the perovskite film was characterized using a Zeiss CrossBeam 1540XB FESEM (equipped with an in-lens detector). An accelerating voltage of 5 kV was used for imaging.

X-ray diffraction: The crystallography of the films was investigated using Bruker D8 Discover (equipped with Lynxeye XE detector, and Cu Kα is 0.15418 nm)

UV-Vis spectrum: The absorbance spectrum was measured by Cary5000 (Agilent technologies) in a 150 mm integrating sphere from 400-850 nm.

Kelvin probe force microscope: KPFM measurment was performed on MFP-3D atomic force microscope (Asylum Research) with a Ti/Ir coated conductive tip (ASYELEC.01-R2) under dry air environment. The tip potential was measured using a mounted HOPG sample (Veeco).

Photo-electron Spectroscopy in Air: The valence band position of perovskite samples was measured by PESA performed by a AC-2 instrument (Riken Instruments). The measurement was conducted at 5 nW excitation light power and scanned from 4.5 eV to 6.2 eV with a step of 0.05 eV. The 0.33 power of yields against excitation energy was plotted and a linear fit was performed to extract the takeoff energy.

The X-ray photoelectron spectroscopy: XPS measurements were carried out in ultra-high vacuum conditions ($<10^{-10}$ mbar) using standard Omicron multi-probe XPS system with Al Kα 1486.7 eV monochromatic X-ray source, Argus hemispherical electron spectrometer and 128 channels MCP detector. Samples were air exposed before the XPS measurements. CASA-XPS software was used for data analysis and curve fitting. The binding energy of the high resolution core levels was calibrated using C 1s as reference.

The impedance spectroscopy: A Metrohm Autolab PGSTAT 302N was used for IS measurements. The solar cell was placed in a cryostat (OptistatDN-V, Oxford Instruments) with the pressure $< 1\times10^{-5}$ mbar. The cryostat was placed in a grounded aluminum box forming a Faraday cage to reduce electronic noises from outside and block the background illumination.

Measurements were performed using the Metrohm software Nova 2.1. All measurements were performed using a perturbation voltage amplitude of 10 mV from 1 MHz to 1 Hz.

The photoluminescence measurements: The PL spectra were recorded in a FluoTime 300 photoluminescence lifetime and steady state spectrometer (PicoQuant). The illumination source was a 485 nm picosecond laser diode head. And a 575 nm filter was inserted between the sample and the detector to block scattered or reflected laser. The sample was placed in a N_2 filled quartz holder to prevent contact with moisture during the measurement.

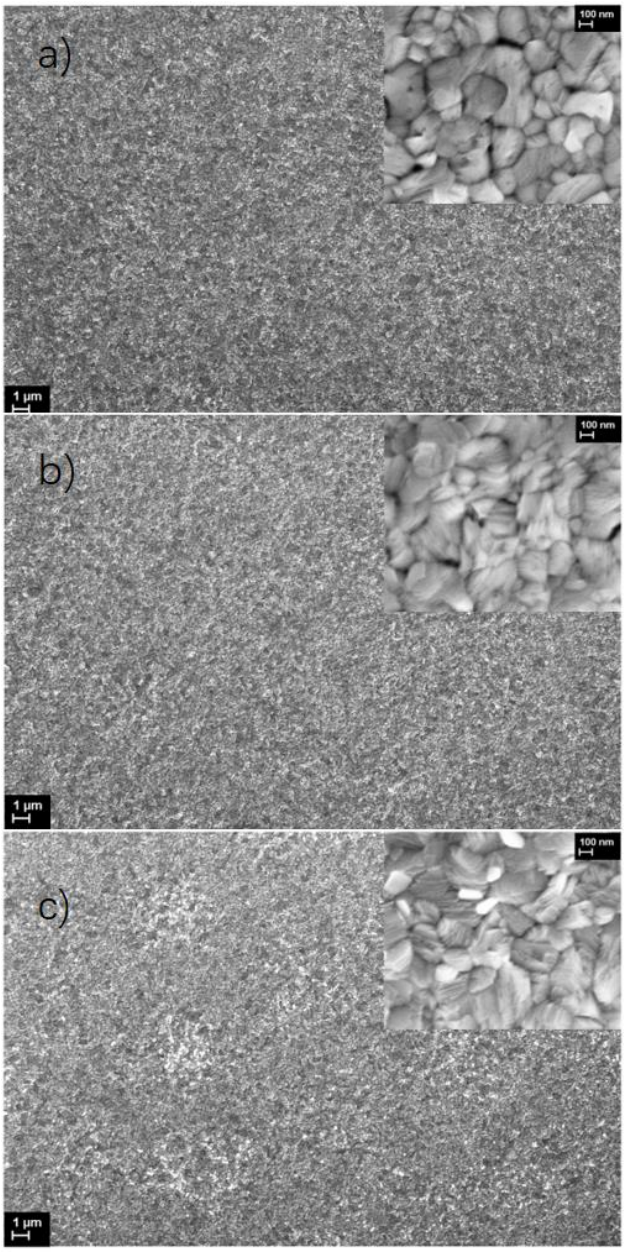

Figure S1: The top-view morphology of (a) 90-in, (b) 90-out and (c) 100-out sample respectively. Inset shows the zoom-in morphology at higher magnification.

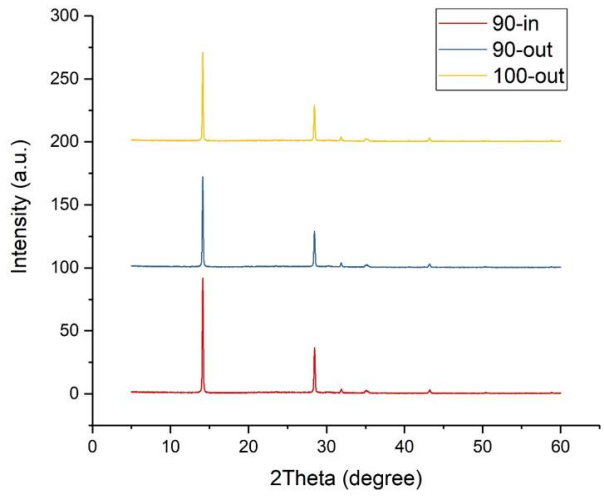

Figure S2: The XRD spectra of 90-in, 90-out and 100-out samples.

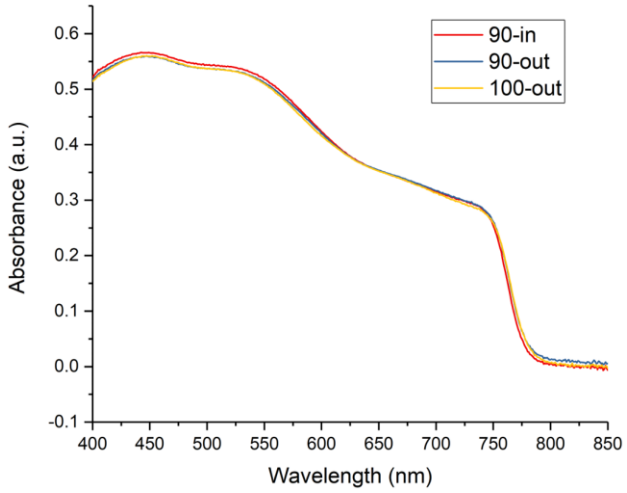

Figure S3: The UV-Vis absorbance spectra of 90-in, 90-out and 100-out samples.

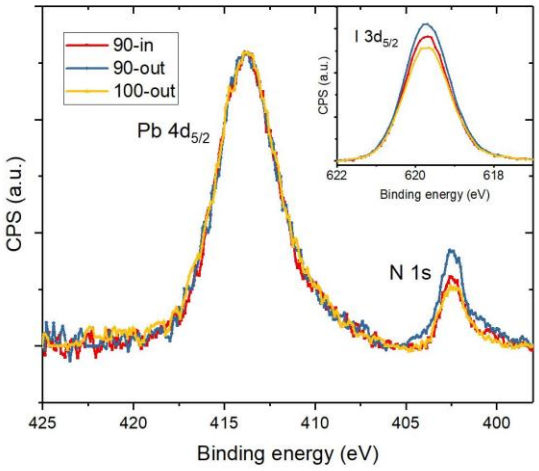

Figure S4: The XPS spectra of the 90-in, 90-out and 100-out samples. All spectra have been normalized based on the Pb $4d_{5/2}$ peak to remove any signal intensity deviation caused by systematic errors.

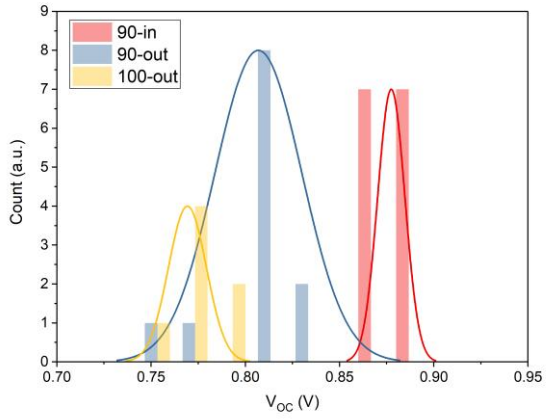

Figure S5: The statistical distribution of the V_{OC} of 90-in, 90-out and 100-out samples.

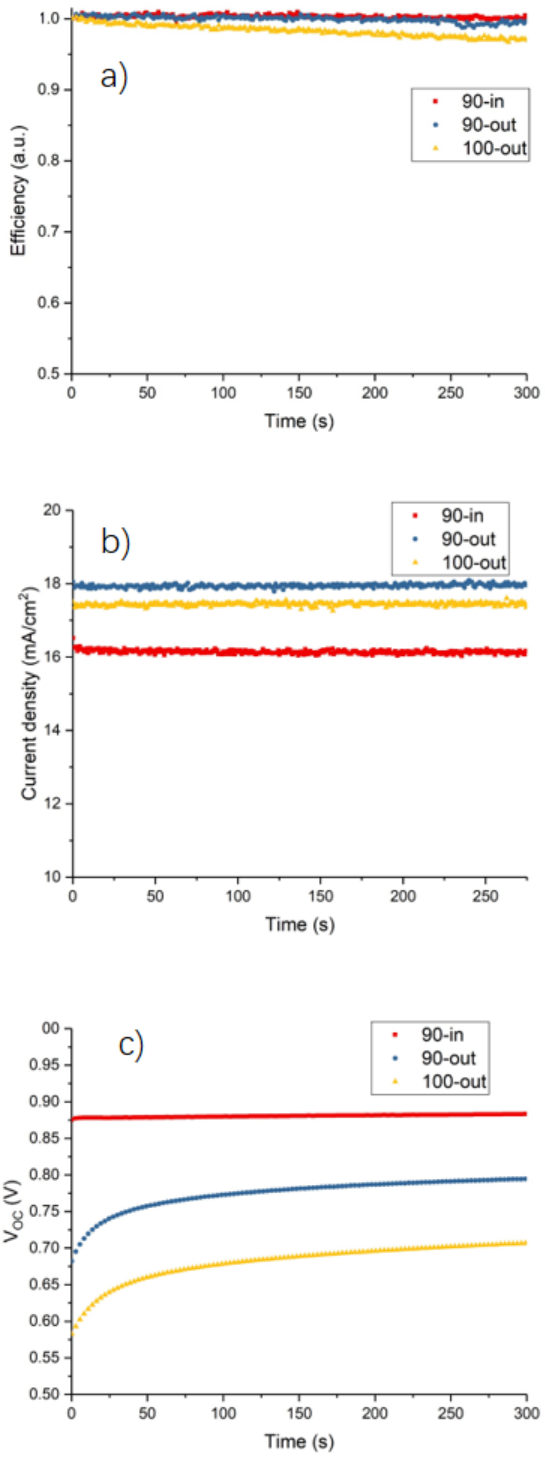

Figure S6: The tracking curves of 90-in, 90-out and 100-out samples, including: (a) normalized efficiency, (b) J_{SC} and (c) V_{OC}. These measurements were performed successively.

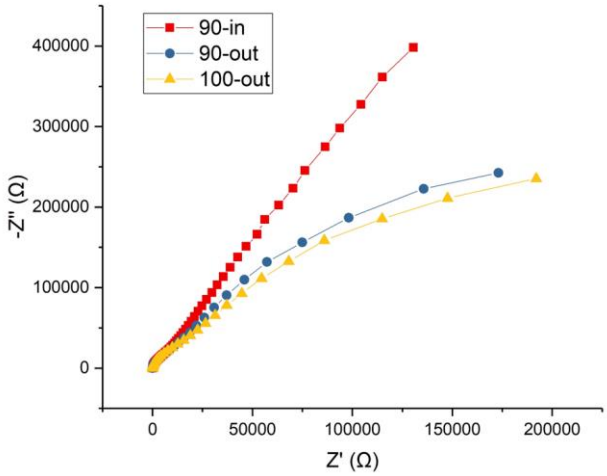

Figure S7: The impedance measurements of the 90-in, 90-out and 100-out samples under dark at 0.3 V. The smaller bias is chosen to prevent potential interference from ion redistribution.

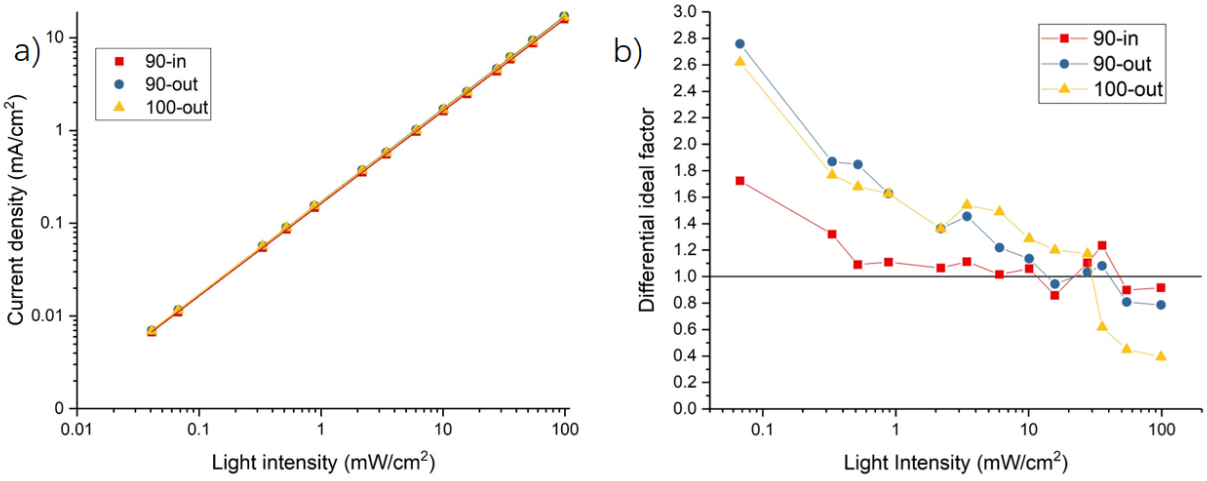

Figure S8: (a) The light intensity dependent measurement of J_{SC}. The extracted α value according to $J_{SC} \propto I^{\alpha}$ is 0.996, 0.999, 0.997 for 90-in, 90-out and 100-out sample respectively. (b) The differential ideal factors for the 90-in, 90-out and 100-out samples. The reference line at ideal factor 1 is drawn to guide eyes.

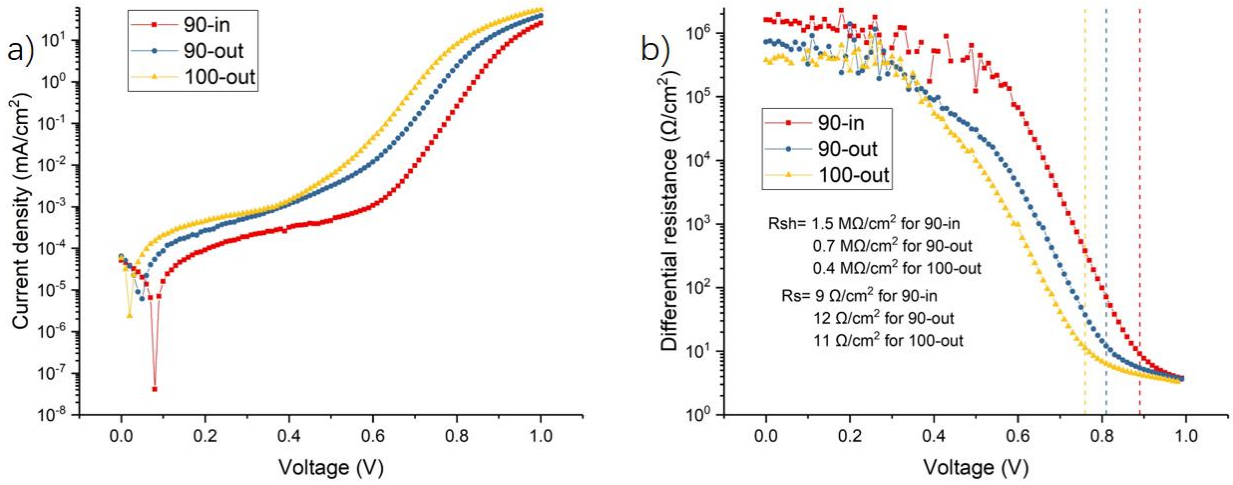

Figure S9: (a) The semi-log dark J-V curves of the 90-in, 90-out and 100-out samples. (b) The differential resistance derived from the dark J-V curves. The shunt resistance (Rsh) is extracted at the short circuit condition while the series resistance (Rs) is at the V_{OC} points (as indicated by the colored dash lines). The resistance values are listed in the graph.

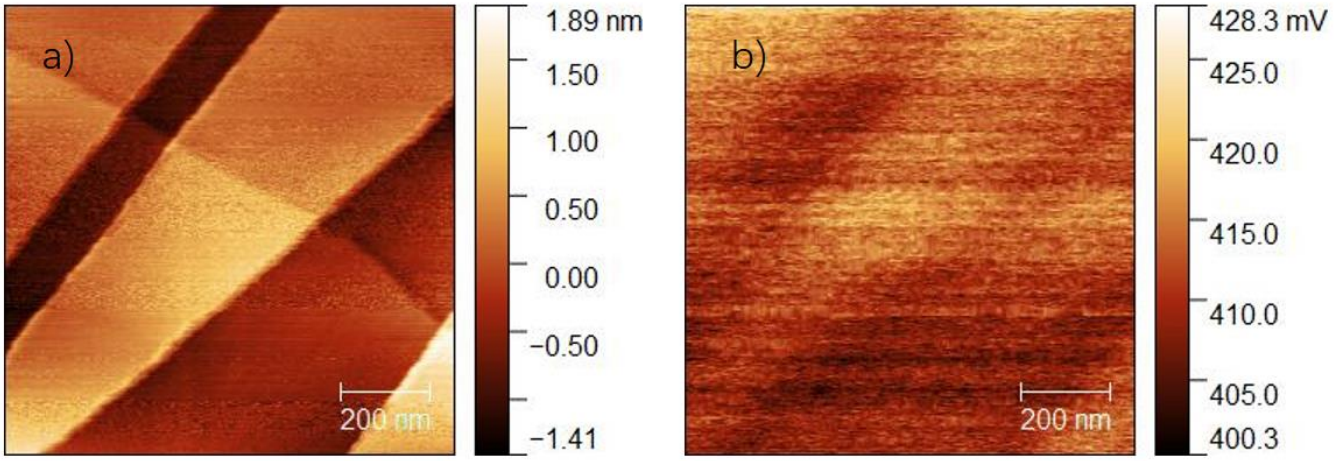

Figure S10: The (a) topography image and (b) potential profile of HOPG measured by KPFM. The RMS roughness is 0.56 nm, the mean potential is around 415 mV with 3.6 mV RMS. Based on the reported HOPG work function of -4.6 eV, the tip work function was calculated to be -5.015 eV.[1]

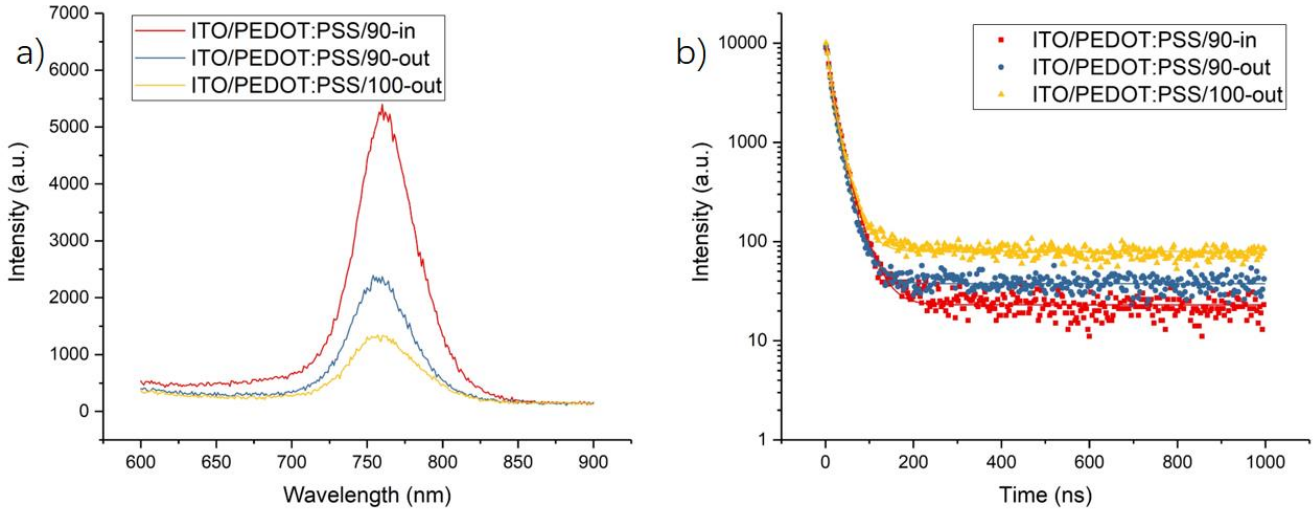

Figure S11: The (a) static spectra and (b) dynamic curves of the PL measurements on 90-in, 90-out and 100-out samples on PEDOT:PSS substrates.

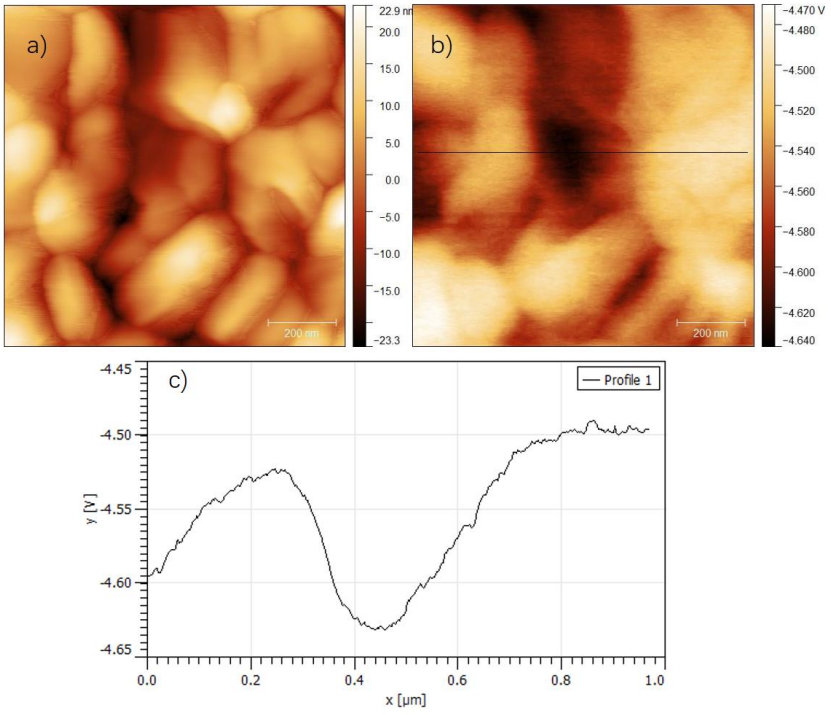

Figure S12: The KPFM image of 90-in sample with (a) topography, (b) potential profile and (c) line potential profile. The line is pointed in Figure (b) and over 100 mV potential difference is observed across grains.

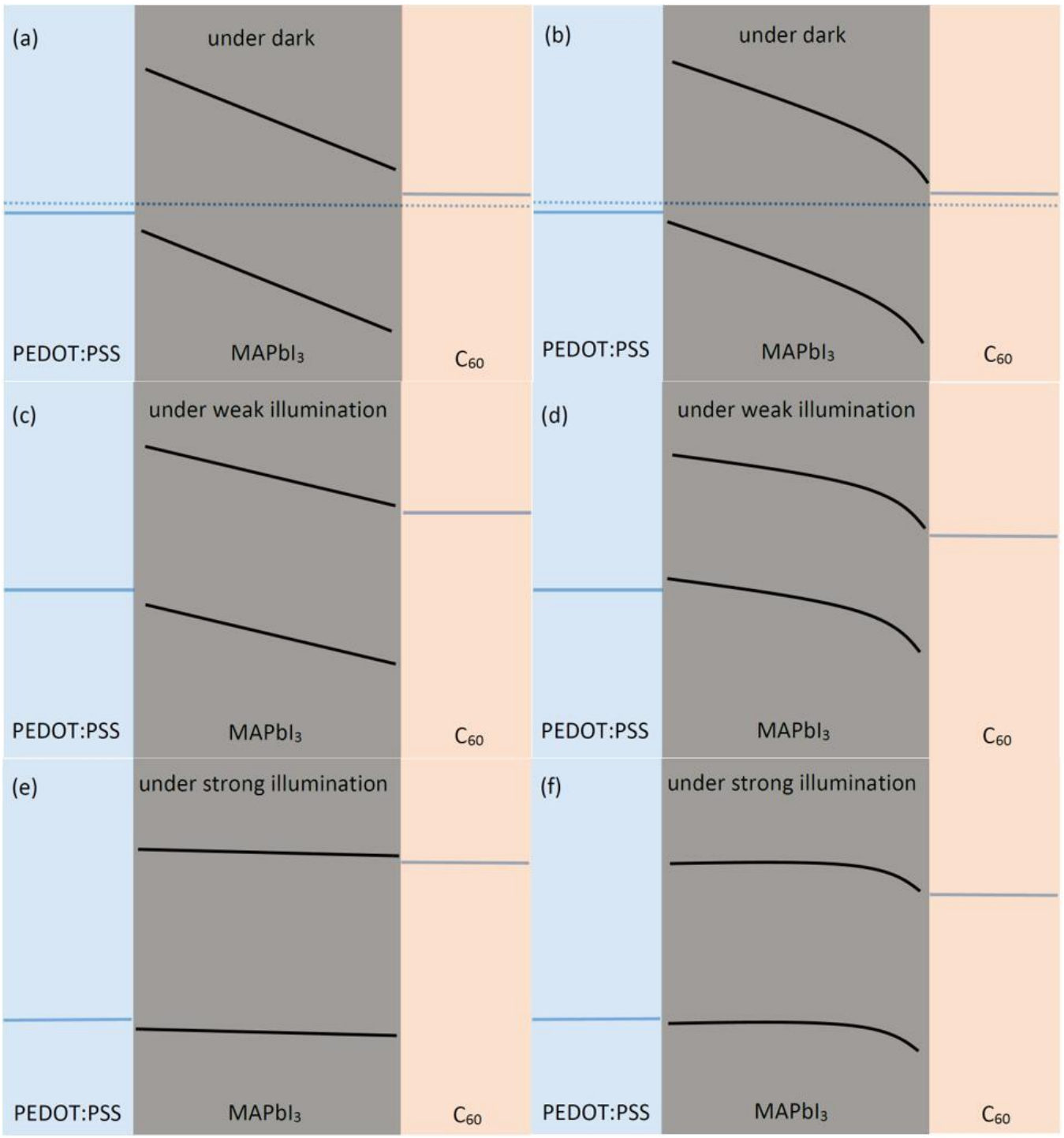

Figure S13: Diagram of band structure at open circuit condition without (a)(c)(e) and with (b)(d)(f) surface band bending. The downward bending diagram is given according to the KPFM and PESA characterization results. (a-b) shows the open circuit band structure in the dark, the dashed blue line indicates the Fermi level across the device; (c-d) shows the open circuit band

structure under lower light intensities. With surface band bending, the reduced built-in field in bulk perovskite leads to suppressed charge transport, which results in lower V_{OC}; (e-f) shows the open circuit band structure at higher light intensities. The bulk built-in field in perovskite layers is too weak to sustain efficient charge transport and injection.

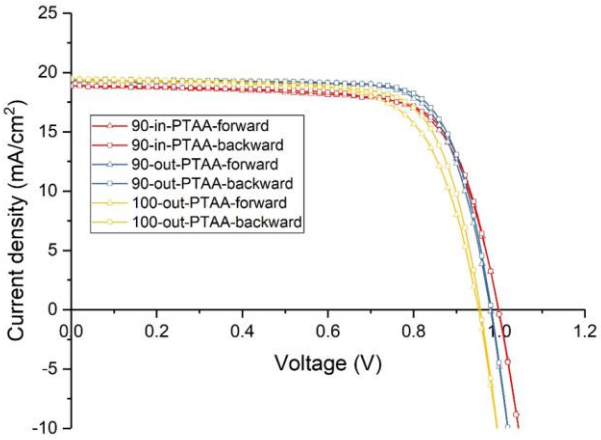

Figure S14: Forward and backward J-V scans of 90-in, 90-out and 100-out samples with the PTAA/$MAPbI_3$/C_{60} architecture. The V_{OC} of 90-in sample is 0.998 V, 90-out 0.982 V, and 100-out 0.956 V.

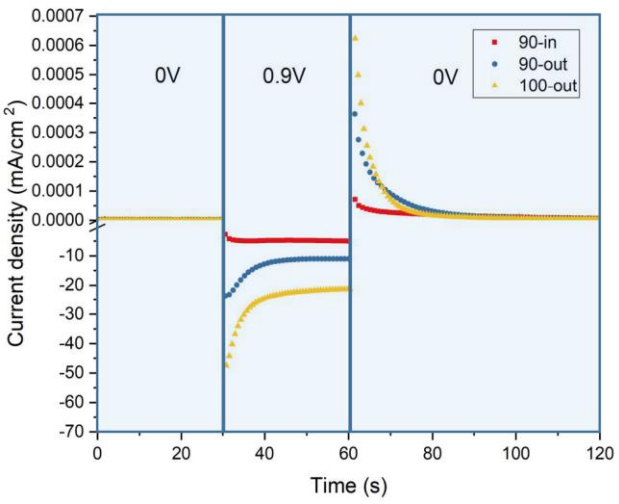

Figure S15: The transient ionic results of 90-in, 90-out and 100-out device samples. The movable ion density was calculated to be 1.4 x 10^{17} cm^{-3} for 90-in, 4.6 x 10^{17} cm^{-3} for 90-out and 5.5 x 10^{17} cm^{-3} for 100-out sample, respectively.

1. Garrillo, P. A. F.; Grévin, B.; Chevalier, N.; Borowik, Ł., Calibrated work function mapping by Kelvin probe force microscopy. Rev. Sci. Instrum. 2018, 89, 043702.